



**Stimuli-Responsive/Rheoreversible Hydraulic Fracturing
Fluids as an Alternative to Support Geothermal and Fossil
Energy Production**

Journal:	<i>Green Chemistry</i>
Manuscript ID:	GC-ART-10-2014-001917.R2
Article Type:	Paper
Date Submitted by the Author:	18-Mar-2015
Complete List of Authors:	<p>Jung, Hun Bok; Pacific Northwest National Laboratory, Energy and Environment Directorate Carroll, Kenneth; NMSU, Plant & Environmental Science Kabilan, Senthil; Pacific Northwest National Laboratory, Fundamental and computational science directorate Heldebrant, David; Pacific Northwest National Lab, Hoyt, David; Pacific Northwest National Laboratory, Environmental Molecular Sciences Laboratory Zhong, Lirong; Pacific Northwest National Laboratory, Energy and Environment Directorate Varga, Tamas; Pacific Northwest National Laboratory, Environmental Molecular Sciences Laboratory Stephens, Sean; Pacific Northwest National Laboratory, Environmental Molecular Sciences Laboratory Adams, Lexor; Pacific Northwest National Laboratory, Environmental Molecular Sciences Laboratory Bonneville, Alain; Pacific Northwest National Laboratory, Energy and Environment Directorate Kuprat, Andrew; Pacific Northwest National Laboratory, Biological Sciences Division Fernandez, Carlos; Pacific Northwest National Laboratory,</p>

ARTICLE

Stimuli-Responsive/Rheoreversible Hydraulic Fracturing Fluids as an Alternative to Support Geothermal and Fossil Energy Production

Cite this: DOI: 10.1039/x0xx00000x

Received 00th October 2014,
Accepted 00th November 2014

DOI: 10.1039/x0xx00000x

www.rsc.org/H. B. Jung,^a K. C. Carroll,^b S. Kabilan,^a D. J. Heldebrant,^a D. Hoyt,^a L. Zhong,^a T. Varga,^a S. Stephens,^a L. Adams,^a A. Bonneville,^a A. Kuprat^a and C. A. Fernandez^{a*}

Cost-effective yet safe creation of high-permeability reservoirs within deep bedrock is the primary challenge for the viability of enhanced geothermal systems (EGS) and unconventional oil/gas recovery. Although fracturing fluids are commonly used for oil/gas, standard fracturing methods are not developed or proven for EGS temperatures and pressures. Furthermore, the environmental impacts of currently used fracturing methods are only recently being determined. Widespread concerns about the environmental contamination have resulted in a number of regulations for fracturing fluids advocating for greener fracturing processes. To enable EGS feasibility and lessen environmental impact of reservoir stimulation, an environmentally benign, CO₂-activated, rheoreversible fracturing fluid that enhances permeability through fracturing due to in situ volume expansion and gel formation is investigated herein. The chemical mechanism, stability, phase-change behavior, and rheology for a novel polyallylamine (PAA)-CO₂ fracturing fluid was characterized at EGS temperatures and pressures. Hydrogel is formed upon reaction with CO₂, and this process is reversible (via CO₂ depressurization or solubilizing with a diluted acid) allowing potential removal from the formation and recycling, decreasing environmental impact. Rock obtained from the Coso geothermal field was fractured in laboratory-scale experiments under various EGS temperatures and pressures at significantly (at least an order of magnitude) lower effective stress than standard fracturing fluids, and the fractures were characterized with imaging, permeability measurement, and flow modeling. Although additional work is required to further understand the fluid properties, potential and limitations, this novel fracturing fluid and process represent a potential alternative to conventional fracturing fluids to vastly reduce water usage and the environmental impact of fracturing practices and effectively make EGS production and unconventional oil/gas exploitation cost-effective and cleaner.

Introduction

The urgent need for alternative renewable energy sources is well recognized. Geothermal heat recovery is among the cleanest energy sources, only requiring drilling of a well, a circulation pump and a generator. Enhanced geothermal systems (EGS) are reservoirs created by stimulation or fracturing where there is hot rock but insufficient natural permeability. If EGS can be developed, geothermal has promise to become a significant alternative for energy production both within the United States and worldwide.[1, 2] As a renewable energy alternative, geothermal is a stable source with low CO₂ emissions, thus helping to mitigate climate change. However, to our knowledge, no prior EGS project has sustained production at rates greater than 50% of what is needed for economic viability. The reason for a lack of sustained production is the tremendous amounts of fractured-rock surface area for heat exchange and high fluid flow rates needed to sustain EGS.[3]

Indeed, the primary limitation for commercial EGS is the current inability to cost-effectively create high-permeability reservoirs from impermeable, crystalline rock located within the 900–4000 m depth range in a temperature range of 150 - 400 °C.[2] Recent advances in hydraulic fracturing techniques and horizontal drilling represent a key driver for EGS development. This is not different from unconventional oil and gas exploitation where hydraulic fracturing has been implemented in over 52,000 oil and gas wells across the U.S. to extract more than 50 years' worth of unconventional domestic fossil fuels as conventionally recoverable reserves decline.[4-6]

Hydraulic fracturing processes utilize brute force, hydraulic pressure, from millions of gallons of water per well that are pumped down the wellbore at high pressures to create a network of cracks in the source rock. Three different concepts exist for hydraulic stimulation of a reservoir, depending on rock, formation and fluid properties namely hydraulic proppant fracturing (HPF), water

fracturing (WF), and hybrid fracturing (HF). HPF employs highly viscous gels with high proppant concentrations creating highly conductive, but relatively short fractures in a permeable reservoir. The fracture connects the well and the reservoir and reduces permeability impairments in the direct vicinity of the well (commonly referred to as skin), which results in a productivity increase. After fracture generation and proppant pack emplacement are completed, the well is shut-in for some time to allow the fluid to leakoff into the formation and the pressure declines. During this shut-in phase, the fracture closes partially fixing the proppant pack in place.[7] The second fracturing approach, WF consist of introducing water containing friction-reducing chemicals (slick water) partially with added low proppant concentration (mainly sieved sand) to create long and narrow fractures. WF treatment aims at connecting reservoir parts at some distance from the bore hole. In addition in-flow area is maximized by connecting the well to a network of natural joints. In geothermal hot dry rock applications, WF treatments are applied to connect two wells in a tight hard rock (e.g. granite).[8] The HF method consists on a number of combinations of fracture stimulations using cross-linked gels, linear gels, and slick water fluids. Hybrid fracturing combines the advantages of HPF and WF treatments by combining an initial slick water phase to create the fracture geometry. This process is then followed by a cross-linked gel treatment that allows carrying the proppant load to the far end of the induced fracture. The geometry of the created fracture network differs from that of a conventional HPF stimulation design. For example, the fractures are considerably longer compared to HPF and the effective propped fracture length is higher.[9] Proppants commonly used in unconventional (tight) oil and gas recovery include sand and ceramic beads while in geothermal systems bauxite and resin-coated bauxite and ceramics are the standard due to their high thermal stability.[10-12] Rheological modifiers, which account for approximately 1 wt% of the fracturing fluid, include gellants (0.5%) to suspend proppants, acids (0.07%) to dissolve minerals and initiate fractures, corrosion inhibitors (0.05%), friction reducers (0.05%) to lubricate fissures, clay control (0.034%), crosslinkers (0.032%), scale inhibitors (0.023%), breakers (to delay breakdown of the gels, 0.02%), iron control modifiers (0.004%), and biocides (0.001%).[13] Among the industry standard practices, surfactants and macropolymers (e.g., sodium dodecyl sulfate [SDS] or xanthan gum) are employed to reach fracture pressures. Although in small concentration, there have been fears that the additives could contaminate surface aquifers.^{2, 3, 6} Furthermore, macropolymers developed for accessing oil/gas may not be applicable at geothermal temperature ranges (>150°C) due to thermal decay.[14-16] They are also difficult to remove from the formation after fracture creation. The residue of injected polymers and drilling mud not removed during fracture cleanup, called fracture skin, limits hydraulic fracturing production enhancement because it decreases flow rates and heat transfer in EGS. A key issue related to hydraulic fracturing technology is the volume of wastewater that must be disposed of. This is particularly true for EGS due not only to the chemicals employed in the fracturing fluids but the amount of minerals, including radium, arsenic, barium, strontium and uranium, extracted at high temperatures during reservoir stimulation.^{2, 3, 6, 17}

The large volumes and chemical content of hydraulic fracturing wastewater have stoked public fears of water and soil contamination and have generated both environmental and economic concerns.⁶ As a result, 21 US states have adopted mandatory rules including the implementation of risk/toxicity assessments and chemical-disclosure registries for the chemical mixtures used while the European Union is phasing in a unified chemical-regulation programme that governs reporting across all commercial sectors. Finally, there is a strong

need for optimization of fracture creation/propagation and permeability enhancement due to the excessive costs related to well drilling and completion [a typical well budget averaged \$7.5 million (drilling plus completion) in early 2011]. These are areas of evolving research in hydraulic fracturing and, despite the limited understanding of stimulation in geothermal systems, it is clear that permeability-enhancement technologies must be developed to make EGS viable.[2, 3, 17]

We postulated that a stimuli-responsive fracturing fluid that can mediate a stimulated (chemically-activated) expansion in confined environments could provide a controllable increase of hydraulic pressure to aid in fracturing processes. *In situ* controlling of the rheological properties of the fracturing fluid would dramatically enhance permeability increase in EGS. The challenge in developing such reactive hydraulic fracturing fluids is that the material has to be nontoxic and inexpensive, and the chemical stimulus must be readily available. CO₂-activated materials could be the answer in developing these novel fracturing fluids, as CO₂ is nontoxic, inexpensive, and readily available as trapped gas inside geological strata. Additionally, key process infrastructure is available as it is currently used for similar technologies such as enhanced oil recovery (EOR). Furthermore, rheoreversibility (e.g., liquid to gel and gel to liquid) would make these materials easy to recover from the formation, which would decrease potential environmental impact and, as importantly, the resulting increase in flow rates and heat transfer would accelerate geothermal energy production.

The objective of this study is to reduce environmental impact yet enhance the economic viability of EGS by developing a CO₂-activated hydraulic fracturing fluid to be used for reservoir creation and fracture stimulation. We introduce for the first time in this field proof of concept towards the development of a novel and potentially recyclable hydraulic fracturing fluid that undergoes a chemically-induced large and very rapid volume expansion with a simultaneous increase in viscosity triggered by CO₂ at temperatures relevant for reservoir stimulation in EGS. The volume expansion, which will specifically occur at EGS depths of interest, generates an exceptionally high “spike” in the fluid pressure and a resulting mechanical stress in fracture networks of highly impermeable rock enabling the initiation of fractures at effective stress at least an order of magnitude lower than current technology. Although there are reports on CO₂-induced formation of hydrogels, [18-26] the reported fracturing fluid shows for the first time a stimuli-responsive large and reversible volume expansion which occurs at temperatures and pressures relevant to EGS. The proposed fluid addresses two of the potential environmental aspects of subsurface fracturing processes. The first one is the number and concentration of chemical additives introduced in the water with the potential ground and aquifer contamination. This fracturing fluid decreases the number of chemical additives introduced in the subsurface such as rheology modifiers (e.g. xanthan gum, surfactants, gels), biocides (e.g. chlorine) and corrosion inhibitors (e.g. formic acid). These additives will not be required due to the modulated volume and viscosity of the fracturing fluid as well as to its antioxidant[27] and biocide nature.[28] The second environmental issue is the impact of produced waste water due to the millions of gallons of water used during stimulation processes. The CO₂-triggered volume expansion, as it will be discussed later, reduces the energy requirements for fracture creation/propagation (reducing greenhouse gas emissions) due to the pressure spike created in confined environments that aids to the hydraulic pressure. In addition, the rheoreversible properties of the fluid will facilitate fracture clean-up. As a result, the use of surfactants (such as SDS), cross linkers and breakers will not be required. Furthermore, as will be described later, due to the rheoreversible nature of the fracturing fluid this fluid can be

recovered as an aqueous solution or emulsion and recycled. This is another big benefit of this technology which makes it more environmentally friendly than current fracturing practices.

Three control experiments were performed at identical pressure/temperature conditions. These were pure water, 1 wt% aqueous solutions of SDS and 1 wt% aqueous solutions of xanthan gum. When CO₂ was introduced into 1 wt% aqueous solutions of xanthan gum, 1 wt% aqueous solutions of sodium dodecyl sulfate (SDS), and pure water, the solutions showed no obvious volume expansion, viscosity increase (with exception of SDS that showed a slight viscosity increase) or fracture creation/propagation on EGS rock cores. The reported fracturing fluid technology could replace currently used chemicals and make EGS competitive with hydrocarbons in the energy market and unconventional oil/gas exploitation cost-effective and cleaner. The assessment of key physical and thermodynamic property changes at the elevated temperature and pressure ranges required for EGS operations demonstrates that the hydrogel is stable at temperatures as high as 400 °C representing an excellent candidate for reservoir stimulation in EGS. The hydrogels form with a concomitant significantly rapid (seconds) volume expansion and increase in viscosity, and the process is completely reversible. Laboratory-scale hydraulic fracturing experiments on rock cores from a geothermal field (the Coso geothermal reservoir) were successfully conducted using an aqueous polyallylamine (PAA)-CO₂ fluid system and conventional fracturing fluids, demonstrating the potential of this new technology.

Experimental

High-pressure (HP), high-temperature (HT) experimental setup

The experimental system consisted of a HP cell (internal volume: 11 mL, max. pressure: ~830 atm, max. temperature: ~400 °C) manufactured by Pacific Northwest National Laboratory, an HP generator (standard laboratory model, High Pressure Equipment Company), a syringe pump (Teledyne Isco, model 260D), as well as a camera (Panasonic) and a monitor (Sony) (Fig. S1). The HP cell was covered by insulation (Thermo Craft Insulation) and was heated using a hot plate (Corning, model PC-420D). The temperature was monitored using a thermocouple (Watlow Electric Manufacturing Company; max. temperature: 1700°C, accuracy: ±2°C) connected to a thermocouple controller (Parr Instrument Co., Parr 4843; operating range: 0–800°C, accuracy: ±2°C). The pressure of the cell was monitored using two pressure gauges (Span Instruments: 0–200 atm, accuracy: ±1% full scale; WIKA Instrument: 0–670 atm, accuracy: ±0.5% full scale), which were connected to the HP generator and the HP cell. The HP cell has three sapphire windows, one on the top and two on the sides (Fig. S2). A small stirring bar was added to stir the polymer solution at 160 rpm. The camera monitoring through a window was used to determine the volume change and observe changes in phase behavior during the reaction with CO₂ at HP and HT conditions.

Rheology monitoring of polymer-CO₂ fluids for reservoir stimulation in EGS

To select a polymer that can react with CO₂ in aqueous media and transition to a volume-expanding viscous hydrogel at pressure and temperature conditions found in EGS, four polymers (Gelest Inc. and Sigma Aldrich) were tested over a range of HP and HT conditions after 20 times dilution with deionized water (DIW) (Table S1). The tested polymers include 3 [(2-Aminoethyl)amino] propylmethoxysiloxane dimethylsiloxane copolymer with 2–4% amino content, 3 aminopropylmethylsiloxane-dimethylsiloxane copolymer with 6–7% amino content, 3 aminopropyl-terminated

polydimethylsiloxane with 3.2–3.8% amino content, and poly(allylamine) solution (average MW ~17,000, 20 wt% in H₂O). Before adding a polymer solution to the HP cell, the cell was heated to approximately 350–370°C (calibrated internal temperature; Fig. S3). The diluted polymer solution was then added to the HP cell using a HP generator (standard laboratory model, High Pressure Equipment Company) up to ~40–50% of total cell volume. After equilibration of the polymer solution at the internal temperature of 353–372°C, CO₂ was injected into the cell by opening a valve connected to a syringe pump at 110 atm. The CO₂ pressure was increased in 10 atm steps until the pressure in the cell reached 300 atm. After equilibrating the system (i.e. no CO₂ flow and pressure variation) at 300 atm for ~10 minutes, the heat was turned off. As the temperature decreased to below 200°C, the venting valve connected to the pressure cell was slowly opened and the reacted polymer solution was collected into a 20-mL vial. After CO₂ was all vented from the HP cell, DIW was added to the cell to remove any remaining polymer solution and clean the inside. The cleaning procedure was repeated several times before a new experiment. Additional experiments on the reaction between 1 wt% PAA solution and CO₂ were conducted at internal temperatures ranging from approximately 60 to 400°C and pressures between 110 and 300 atm to understand the effects of temperature and pressure on the rheology of the PAA solution during the reaction with CO₂. The HP cell was filled with 1 wt% PAA solution up to ~40–50% of the total cell volume (the level in the window indicated the filling percent) before injecting CO₂ at a range of internal temperatures, namely 58, 127, 196, 265, 333, and 402°C. Prior to the CO₂ injection, the internal pressure of the HP cell containing PAA solution was below 1 atm at temperatures of 58–196 °C, and approximately 40, 70, and 150 atm at temperatures of 265, 333, and 402°C, respectively.

Viscosity measurements

The rheology properties of the 1 wt% PAA solution, the 1 wt% sodium dodecyl sulfate (SDS) solution (control experiment), and the 0.1% xanthan gum solution (control experiment) at constant temperature (190°C) and incremental CO₂ pressure (up to 135 atm) were determined using an Anton Paar Physica MCR101 rheometer equipped with a C-PTD200 Peltier temperature control system and a pressure cell (CC25/PR150, temperature and pressure limits 200°C and 140 atm). Xanthan gum was diluted 10 times with respect to the other two compounds in order to begin the analysis with similar viscosity values to PAA and SDS 1 wt%. The rheology of a DIW and CO₂ mixture under similar temperature and pressure conditions (another control experiment) was also determined for comparison to the fluid systems.

Before rheology measurement, the measuring system and the pressure cell were coupled and the rheometer motor was adjusted. A bearing/air check was conducted to evaluate the conditions and performances of the bearings in the head of the pressure cell. For the measurement, the pressure cell (vol. = 26 mL) was first preheated to 90°C. Water or a chemical solution (13 mL) was then injected into the cell through a port and the temperature increased to 190°C. The cell was sealed and CO₂ was injected into the cell using a syringe pump in steps of about 6 atm to a final pressure of 135 atm with minimum variation in temperature. The rheology measurement at a fixed shear rate (100 s⁻¹) was started immediately after CO₂ was introduced. Finally, a measurement of viscosity as a function of shear rate from 3 to 120 s⁻¹ was conducted at 190°C and 135 atm on all fluid mixtures.

In situ HP and HT magic angle spinning nuclear magnetic resonance (MAS-NMR) analysis

In situ HP MAS- ^{13}C NMR analysis has been previously described by our group.[29, 30] Briefly, specially machined HP rotors of 7.5 mm outer diameter (OD) and 6.0 mm inner diameter (ID) and with a sample capacity of 450 μL were used. These rotors were equipped with a valve to allow controlled exposure of the sample to pressurized CO_2 . Firstly, and in order to optimize experimental conditions, supercritical CO_2 (sc CO_2) at 150°C and 120 bar was injected and its NMR spectrum collected. The rotor was then purged and 200 μL of a 1 wt% PAA solution was introduced. The rotor was sealed and sc CO_2 at 72°C and 86 atm was injected. In situ NMR spectra of the fluid system were collected in the temperature range of 72–154°C. The HP-MAS sample rotor was loaded into a previously described HP NMR rotor reaction chamber (internal volume: 27mls)[29] and was temperature regulated within a temperature controlled oven ($\pm 0.1^\circ\text{C}$, Thermal Product Solutions, Model DC-256) and monitored by two independent thermocouples within the HP-MAS rotor reaction chamber. Pressure transducers in a dual 260 mL syringe pump (Teledyne-ISCO-model 260D) reported pressure with a pressure resolution of ± 1 psi. For the NMR investigation, before the HP-MAS sample rotor was loaded into the HP-MAS rotor, research grade 99% ^{13}C -labeled CO_2 gas (Sigma-Aldrich/Isotech) was mixed with high purity natural abundance CO_2 at a ratio of 1:9, corresponding to a net isotope enrichment of 10%. After careful pre-purging of the reaction chamber and rotor headspace, 10% ^{13}C -labeled CO_2 was then pressurized to 86 atm (1250 psi) and equilibrated at 72°C. The 1 wt% PAA solution and the rotor valve were sealed under pressure after equilibration for 15 minutes, and then transferred to an Agilent-Varian VNMRS spectrometer equipped with an 89-mm bore 7.05 T magnet. Temperature was maintained during transfer in specially constructed sample holders.

All the ^{13}C NMR measurements were performed on an Agilent-Varian 300 MHz VNMRS spectrometer at 75.43 MHz Larmor frequency using a double-resonance 7.5 mm MAS probe capable of 7.0 kHz maximum spinning frequency, in conjunction with a commercially available variable-temperature stack. Using a solid-state ^{13}C NMR high-power decoupling single pulse (SP) experiment, all ^{13}C MAS spectra were collected with a spinning rate of 1.0 kHz, with a 2.0 μsec ^{13}C pulse width (45° flip angle), 5 sec recycle delay; 120–1000 transients were accumulated over a temperature range of 72–154°C. ^{13}C T1 saturation recovery experiments validated the 5 sec recycle time as appropriate. A power level for ^1H decoupling of 31.2 kHz with two-pulse phase-modulated decoupling was employed during ^{13}C signal acquisition (300 msec). 15,000 real points were collected and zero filled to 64,000 points over a 50 kHz sweep width. Spectral apodization using Lorentzian line broadening of 40 Hz and gaussian function of 0.01 Hz was applied before Fourier transformation. The C chemical shifts were referenced using an external standard, adamantane (37.85 ppm).

Hydraulic fracturing experiments

A laboratory-scale hydraulic fracturing experiment was performed using rock cores from the Coso geothermal field in California. Rock samples consisted of Mesozoic diorite metamorphosed to greenschist facies. The raw sample material was cut into small cylindrical rock cores (1.59 cm diameter and 5.08 cm length) and a centered hole (0.32 cm diameter and 2.54 cm deep) was drilled from the top of the cylinder. Stainless steel tubing (0.16 cm OD, High Pressure Equipment Company) was introduced 0.64 cm into the hole leaving an internal dead volume of ~ 200 μL in the rock core (Fig. S4). The connection was sealed with Portland cement slurry (water-to-cement ratio = 0.4), and was cured for over a week. The cement sealing was

to prevent any communication between the external fluid (water) used to apply the desired confining pressure and the internal dead volume in the rock core during the course of the experiment. The cemented rock core (total diameter ~ 2.4 cm) was introduced into the flow reactor (2.64 cm ID, temperature rating: 427°C, pressure rating: 670 atm; High Pressure Equipment Company), the reactor capped, and the tubing communicating with the rock core connected to the HP system via a three-way valve. This valve was used to deliver polymer solution or CO_2 . The reactor was heated using heating tape, and temperature was monitored with a thermocouple controller (Parr Instrument Co., Parr 4843; operating range: 0–800°C, accuracy: $\pm 2^\circ\text{C}$) and a thermocouple (Watlow Electric Manufacturing Company; max. temperature: 1700°C, accuracy: $\pm 2^\circ\text{C}$) attached to the surface of the reactor (Fig. S5 and Fig. S6). Preliminary experiments demonstrated that the temperature inside the reactor is essentially the same as the reactor surface temperature at equilibrium. A vacuum pump was used to remove any air and moisture present in the system before introducing approximately 200 μL of a given solution (1 wt% PAA, 1 wt% SDS, or DIW). After the reactor target temperature was reached (210°C), water was injected into the empty space of the reactor using a manual pump to increase confining pressure and time was allowed for the reactor temperature to reach 210 °C. In order to simplify the experimental setup, the rock sample is maintained under a confining pressure equal to the overburden pressure (or vertical stress). This case corresponds to the isotropic stress regime in actual subsurface conditions where no tectonic forces are acting and where the two horizontal stresses are equal to the vertical stress. CO_2 pressure and confining pressure were monitored using two pressure gauges (pressure range 0–670 atm, High Pressure Equipment Company). Equalization of both pressures was an indication of communication between the rock core and the confining fluid (water) by fracture formation. The confining pressure was first increased to 68 atm, immediately followed by introducing 200 μL of 1 wt% PAA solution and 68 atm of CO_2 inside the core sample via the three-way valve at constant temperature. Then, the confining pressure was raised to 136 atm followed by a similar increment in CO_2 pressure to equalize confining pressure and rock core pressure once again. This procedure was repeated until confining pressure and rock internal pressure reached 204 atm. By maintaining the confining pressure at 204 atm, the pressure at the rock core was gradually increased with CO_2 from 204 atm in intervals of 1 atm until we observed an increase in the confining pressure equalizing the internal rock core pressure due to pressure communication between the internal and external fluids. Finally, the system was slowly depressurized and cooled before the rock core was removed from the flow reactor. For comparison fracturing experiments using DIW/ CO_2 and SDS 1 wt%/ CO_2 were also performed (control experiments). After removing the cement sealing cast, the rock core was subjected to a CO_2 leakage test (~ 6 –7 atm pressure), injection of KI (potassium iodide; 0.3 mg/L) solution, and X-ray microtomography (XMT) scanning to examine the formation and distribution of fractures. An additional experiment was conducted at a higher confining pressure (272 atm) and a similar temperature of $\sim 210^\circ\text{C}$ in order to generate larger volume expansion with 1 wt% PAA and CO_2 , following the same procedure described above.

X-ray microtomography analysis

XMT scans were performed at 120 keV and 160 μA for optimum image quality and contrast. The samples were rotated continuously during the scans with momentary stops to collect each projection (shuttling mode) and minimize ring artifacts. A total of 3142 projections were collected over 360 degrees with 0.5-second

exposure time and 4 frames per projection. Image voxel size varied from 30–35 μ depending on specimen dimensions. Separate scans for the top, middle, and bottom of a rock core (Coso 2-2) decreased image voxel size to 15 μ m. The images were reconstructed to obtain three-dimensional datasets using CT Pro 3D (Metris XT 2.2, Nikon Metrology, UK). For rock sample Coso 2-2, the two parts after fracturing were exactly matched and taped previous to XMT analysis.

Computational Fluid Dynamics (CFD) modeling of hydraulic fractures

CFD simulations were performed to visualize hydraulic fractures and compute the bulk permeability. Detailed description of XMT image segmentation, mesh generation and fluid flow simulations can be found elsewhere.[31, 32] Briefly, the XMT images were filtered using edge-preserving hybrid median filter to remove high frequency noise and the background was normalized to remove any low frequency noise. Intensity thresholds followed by manual validation was performed to identify the fracture boundaries. An isosurface from the segmented data was extracted using a variant of marching cube algorithm[33] and smoothed using volume conserving smoothing.[34] The isosurface was imported in Magics (Materialise, Plymouth, MI, USA) to clean up any intersecting and overlapping triangles and also to create a flat inlet surface for boundary condition specification as it will be shown in the results and discussion section. The outlet boundary in this case was circular representing the interface between the hydraulic fracture in the rock sample and surrounding cement packing. Lagrit-PNNL was used to adapt the triangulated mesh to gradient limited feature size for further scale-invariant meshing.[35] The gradient limited feature size guaranteed a minimum of six tetrahedral elements spanning the narrowest region in the mesh. The volume mesh was produced using the Delaunay approach and to improve the quality of the tetrahedral mesh, a combination of edge flipping and volume-conserving smoothing was used. The final volume mesh consisted of 964480 vertexes, 10022727 faces and 4869231 tetrahedral elements. OpenFOAM (OpenCFD Ltd., Reading, UK), was used to solve the steady state simulation. The flow predictions were based upon the laminar, 3-D, incompressible Navier-Stokes equations for fluid mass and momentum:

$$\nabla \cdot \mathbf{u} = 0$$

$$\frac{\partial \mathbf{u}}{\partial t} + \mathbf{u} \cdot \nabla \mathbf{u} = -\frac{\nabla p}{\rho} + \nu \nabla^2 \mathbf{u}$$

where ρ is the density, ν is the kinematic viscosity, \mathbf{u} is the fluid velocity vector, and p is the pressure.

For all CFD simulations, water at 50°C temperature was considered to be the working fluid (i.e. the fluid that is injected after reservoir completion for heat extraction for energy generation purposes), with a density of 989.15 kg/m³ and a kinematic viscosity of 5.53×10⁻⁷ m²/s. The model was driven by a predetermined bulk flow rate and pressure gradient by setting the velocity magnitude of 0.1 m/s specified at the inlet and a zero pressure boundary condition at the outlet. It is important to note that since the pressure at the outlet is zero, the model adjusts the pressure at the inlet to achieve the correct pressure gradient across the model. Since the velocity is fixed only at the inlet, a resulting varying velocity throughout the model is observed. A no-slip wall condition was applied to the fracture boundaries, which were assumed to be rigid and impermeable.

The intrinsic permeability was calculated using the Darcy's law as given below:

$$q = -k/\mu \times \nabla P$$

where q is the flux (m/s), μ is the dynamic viscosity of fluid (water at 50°C = 5.47×10⁻⁴ Pa·s), and ∇P is the pressure gradient vector (Pa/m).

Results and discussion

CO₂-induced hydrogel formation and fluid volume expansion

The basic concept of this work is to develop reversible CO₂-expanding hydrogels as hydraulic fracturing fluids using CO₂ entrained inside geological formation. Switching to gel from soluble surfactant using CO₂ within the geologic formation during hydraulic fracturing could increase the fluid volume which in turn can provide pressure increases of the fracturing fluid *in situ*. This process may create new fractures and/or extend fracture propagation further into the formation, assuming the hydrogels would form and stabilize at such high temperatures and pressures.

There has been a recent surge in CO₂-reactive materials ranging from solvents, surfaces, catalysts and gels, some of which utilize CO₂ as a chemical trigger.[18, 23, 36-41] Conventional CO₂-reactive liquids degrade thermally and by hydrolysis under geothermal conditions,[18, 23, 38, 39] thus it was required to choose thermally and chemically stable CO₂-reactive polymers. Weiss and others had demonstrated that polyamines, such as amine-functionalized polysiloxanes (PSI), react with CO₂ to form gels at room temperature in a number of organic solvents.[36-38, 42] The group showed that such gels increase their volume and change their rheological properties with CO₂ activation. The gel could then be reversed by removing CO₂ thermally at temperatures as low as 80 °C or by stripping the CO₂ with pH modification.[37, 40] However, these gels (and the resulting volume expansion) did not form in water. To the best of our knowledge there is no report on CO₂-triggered formation of hydrogels resulting in volume expansion in water, which limits dramatically the application of these CO₂-reactive polymers.

In this work four polymers were proposed as potential candidates for reversible CO₂-expanding hydrogels (Table S1) at geothermal temperatures. Aqueous solutions of PAA were the only polymer solutions that successfully formed a viscous hydrogel with corresponding volume expansions in the range of 80–150% during their reaction with CO₂. This is a significant finding, not only because for the first time a CO₂-triggered expanding hydrogel was obtained but also because this hydrogel was stable at temperatures as high as 400 °C (limited by the reactor used). The DOE recently released a report on US EGS which included temperature ranges between 160 °C and 380 °C. Our fluids then represent excellent candidates for reservoir stimulation in EGS since they reproducibly form hydrogels in a temperature range of 196–402°C and CO₂ pressures between 130–300 atm (Fig. S7). The hydrogels formed with a concomitant volume expansion and increase in viscosity (observed by the decrease in fluid convection and movement in the high pressure view cell). Furthermore, this process is reversible as it is described in a later section. In contrast, the other three polymers examined exhibited liquid-like behavior independently of the pressure/temperature conditions.

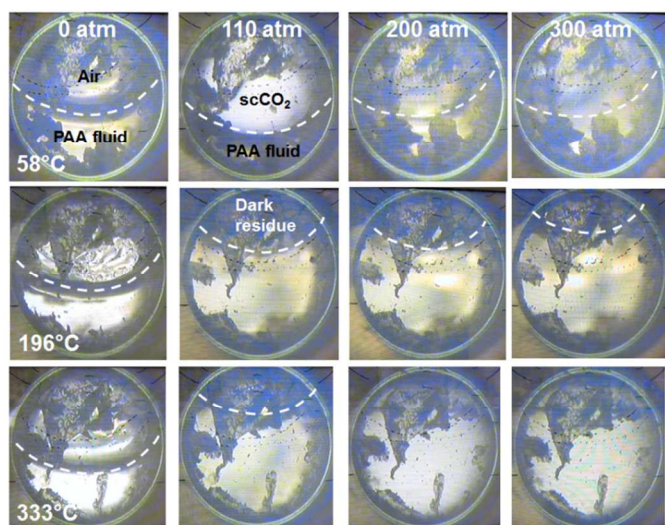


Fig. 1. Volume changes of PAA solution reacted with CO₂ as a function of temperature (58–333°C) and CO₂ pressure (0–300 atm). CO₂ pressure was increased from 0 to 300 atm. The dashed lines indicate the boundary between PAA fluid and supercritical CO₂ (after CO₂ injection) or air/water vapor (before CO₂ injection). The window is partially covered by some residual PAA. Compare these results with Fig. S8 which shows experiment results for DIW/CO₂ in supporting information.

Effect of temperature on the rheology of aqueous PAA-CO₂ fluid system

At temperatures of 58°C and 127°C, the volume expansion of PAA solution was minimal when CO₂ was added to the HP cell at 110 atm. As the CO₂ pressure increased to 300 atm, the volume increased only ~40%. At internal temperatures of 196 and 265°C, there was a volume expansion of ~75 % with CO₂ injection at 110 atm. As the CO₂ pressure increased further, the PAA solution volume increased up to 85% at 300 atm. At internal temperature of 333°C, the volume of the PAA solution had increased 100% at a CO₂ injection pressure of 110 atm, and volume increased to 150% of the original volume above 200 atm. Similar volume expansion was observed at internal temperature of 402°C and at pressures as low as 170 atm (Fig. S7). It is important to mention that the increase in volume was observed only a few seconds after introducing CO₂ at either 110 or 170 atm and that a corresponding increase in the viscosity of the fluid was observed as described in the next section. For example, at internal temperatures ranging from 58 to 265°C, the PAA solution became a viscous liquid, exhibiting low fluid flow. At even higher temperatures, the PAA solution transitioned to a hydrogel in the pressure range of 140–300atm (Fig. 1 and Fig. S7). These results suggest that CO₂ pressure can be employed to precisely control the rheology of PAA solutions, with the potential to create additional stress in confined environments such as during geothermal reservoir stimulation.

Rheology behavior of recycled PAA

To determine whether the recycled PAA maintains the rheological properties in the presence of CO₂, similar experiments were conducted on 1 wt% solutions of recycled PAA obtained from experiments conducted at 300 atm and 330°C. For comparison, experiments with DIW were performed under identical conditions. Pressurizing DIW with CO₂ to 300 atm at 330°C (control experiment) produced minimal volume expansion and active fluid convection similar to DIW before CO₂ injection, suggesting no gel formation (Fig. S8).

Unlike DIW, the 1 wt% PAA solution showed volume expansions of 80%, 85% and 60% after the first, second, and third recycle experiments at 300 atm and 330°C forming a hydrogel in all three cases and at CO₂ pressures as low as 150 atm (Fig. S9). These results illustrate the reversibility of the hydrogel formation and solubilization. During *in situ* fracturing, the removal of the hydrogel through this reoreversible behavior would occur upon either CO₂ depressurization or the introduction of a diluted acid. [38] Bauxite particles or other proppant delivered during fracturing would be used to support fractures after hydrogel removal.[10-12, 43, 44]

These results demonstrate that PAA can be recycled from a gel to an aqueous solution of PAA without irreversible impact on its rheological properties. This is another key feature of these fracturing fluids for mainly two reasons. It suggests that PAA can be removed as an aqueous solution after reservoir depletion and reused dramatically reducing potential environmental impacts and costs during EGS reservoir stimulation given the fact that the process generates millions of gallons of waste water with a large number of chemicals (including hydrocarbons such as benzene, inorganic acids, xanthan gum, ethylene glycol, isopropanol, citric acid, N,N-dimethylformamide, and ammonium persulfate). Additionally, it would accelerate energy production by increasing flow rates and heat transfer.

Viscosity behavior of PAA-CO₂ mixture

Compared to DIW-CO₂, aqueous xanthan-CO₂ and aqueous SDS-CO₂ systems (all control experiments), aqueous PAA-CO₂ fluids appeared to have the highest viscosity and the best rheological performance under the tested conditions. Viscosity of the DIW-CO₂ mixture as a function of pressure is shown in Fig. S10. Viscosity was measured at a shear rate of 100 s⁻¹ and a temperature of 190°C. The viscosity values were relatively constant independently of CO₂ pressure (1–2 cP at 135 atm). Fig. S11 (A1, A2 and A3) compares the viscosity of aqueous PAA-CO₂, aqueous xanthan-CO₂, and SDS-CO₂ mixtures at shear rate of 100 s⁻¹ and 190°C as a function of CO₂ pressure (left plots). The viscosity of the PAA-CO₂ system increases from ~1 cP to 15 cP after CO₂ pressure reached its maximum (instrument limited), 135 atm. This behavior is not observed for xanthan-CO₂ mixture (maximum viscosity 3 cP). In SDS-CO₂ mixtures a somewhat larger viscosity increase was observed with CO₂ pressure (maximum viscosity 6–7 cP) but significantly lower than in the case of PAA-CO₂ mixtures. It is important to mention that all solutions had similar (1-2 cP) viscosity values at 190 °C previous to injecting CO₂. Nevertheless, viscosities of the PAA-CO₂ system were at least 2.5 times higher than the alternative currently used fluids. The viscosity vs. shear rate plots of the fluid systems show shear-thinning behavior in all three mixtures (Fig. S11; B1, B2, B3). Once again the PAA-CO₂ system shows significantly higher viscosity values independently of shear rate. In addition, viscosity values of PAA-CO₂ were an order of magnitude higher at 10 s⁻¹ shear rate than the viscosities measured at 100 s⁻¹ shear rate. These results are of great significance and in agreement with the observed volume expansions of PAA-CO₂ given the temperature and pressure limitations of the rheometer.

In situ Spectroscopic Characterization of PAA-CO₂ mixture

Spectroscopic evidence *in situ* was needed to validate the gel formation and any potential degradation mechanisms. The first spectroscopic characterization of CO₂-reactive gels with PAA was demonstrated *ex situ* by Carretti et al.[36] They showed that the reaction profile for gel formation is initiated when CO₂ reacts with the pendent amines in PAA to initially form carbamate salts, which

then condense to form the corresponding urea, cross-linking the polymer chains. It was believed that the same reaction pathway would be observed under deep geothermal conditions but it was unclear whether carbamate s could survive at HT or if the gel would decompose as amines reacted with CO₂, because carbamate or bicarbonate releases CO₂ at temperatures >120°C [41]. It was hypothesized that the immense pressures of CO₂ could force carbamate formation even at 300°C, but evidence was needed to validate gel formation under deep geothermal conditions.

¹³C Nuclear Magnetic Resonance (NMR) was performed *in situ* to observe the gel formation via speciation of CO₂ and PAA. ¹³C NMR was chosen for this study as there is a high signal-to-noise ratio due to the absence of carbons in the bulk solvent (water), and distinct chemical shifts for carbamates and bicarbonates (155–161 ppm) and dissolved CO₂ (125 ppm). Furthermore, MAS-NMR was performed to probe the speciation of CO₂ with the PAA solutions under HT and HP because MAS allows for increased resolution and line narrowing of polymers compared to conventional solution phase NMR. The *in situ* HP MAS-NMR sample was 200 μL of 1 wt% PAA (40% volume of rotor to allow for potential expansion) prepared in specially machined rotors (7.5 mm OD and 6mm ID)[30] equipped with a valve to allow controlled exposure of the sample to pressurized gas. The sample rotor was loaded into a previously described HP NMR rotor reaction chamber capability.[29] The ¹³C NMR spectra shown in Fig. 2 were obtained at temperatures of 99°C, 127°C and 154°C (A, B, C), which correspond to pressures of 103 bar, 121 bar and 138 bar, respectively, based on previous experiments in the HP cell under analogous conditions. The temperature series of preliminary NMR data suggest the speciation of CO₂ can be confirmed *in situ*. Spectrum A (Fig. 2)

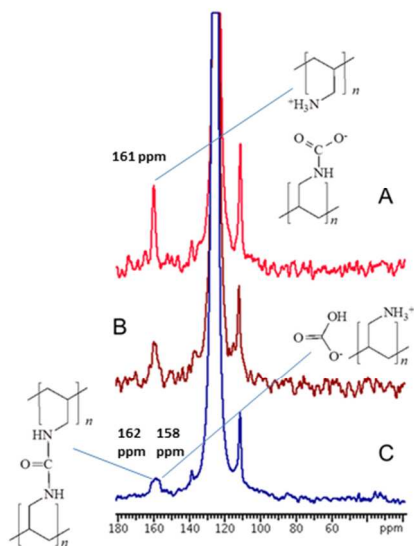


Fig. 2. ¹³C SP-MAS spectra of 1 wt% PAA solution exposed to 10% ¹³C-labeled scCO₂ A: at a temperature of 99°C and a pressure of 103 bar, B: at 127°C and 121 bar, and C: at 154°C and 138 bar using a sample spinning rate of 1.0 kHz. These spectra were acquired with ¹H high power decoupling using a total of 120, 120 and 1000 scans, respectively, with a recycle delay time of 5 s. The ¹³C chemical shifts were referenced using an external reference, adamantane (37.85 ppm).

shows a single peak at 161 ppm (believed to be the carbamate/carbamic acid species) similar to the results of Carretti et al.[36] This peak then transitions into two peaks (Fig. 2, Spectra B and C) of 158 and 162 ppm (potentially overlapped signals), which we assign to the PAA bicarbonate and the cross-linked urea,

respectively. The weathering of these peaks indicates the CO₂ follows the same reaction profile observed by Carretti et al[36] albeit at higher temperatures and pressure, with no signs of decomposition of the PAA (at 127°C and 121 bar). The results of this MAS study are similar to reports of CO₂ adsorption reactions with functionalized amines in nanoporous materials albeit performed *ex situ* (studies in which the relevant high pressures were not maintained during NMR observation).[45] Current equipment limitations prevent NMR measurements at the conditions described above; however refinement of the rotor technology is underway to achieve the 300 bar, 300°C target.

Hydraulic fracturing of rock cores from the Coso geothermal field

Five rock cores from the Coso geothermal field (~490 m depth) were subjected to hydraulic fracturing at ~210°C using 1 wt% PAA and CO₂ (Coso 1-1, Coso 1-2 and Coso 2-2), 1 wt% SDS and CO₂ (Coso 1-3), and DIW and CO₂ (Coso 1-4), the later ones as control experiments. XMT images obtained on the total volumes of the rock cores prior to the experiment indicate that there was no obvious indication of pre-existing fractures at the maximum resolution of the instrument (XMT image voxel size = 30–35 μm; Fig. S12).

Rock samples Coso 1-3 and Coso 1-4 (control experiments)

Hydraulic fracturing experiments with 1 wt% SDS + CO₂ and DIW + CO₂ showed pressure equalization, as an indication of communication between the rock internal dead volume and the confining fluid, at very slow rate (> 3 min) and at pressure differentials (between fracturing fluid pressure and confining pressure) as high as 50 atm which suggests that CO₂ flow to the external confining fluid occurred not through fractures created on the rock core but probably through the cement pores of the shell surrounding the rock core as well as the cement-stainless steel tubing seal. After the experiment, the rock core was removed from the flow reactor and the cement seal was detached from the rock core. CO₂ leakage was not observed on the rock cores Coso 1-3 and Coso 1-4 when CO₂ was injected at 5 atm, verifying no fracture formation and/or propagation in the rock occurred by either aqueous SDS-CO₂ or DIW-CO₂ fluid systems (Fig. S13).

Rock samples Coso 1-1 and Coso 1-2

Experiments performed on samples Coso 1-1 and Coso 1-2 employing 200 μL of 1 wt% aqueous PAA consistently showed communication (fluid flow) between the internal fluid (CO₂/aqueous PAA) and the external confining fluid at effective stress as low as 4 atm followed by rapid (~30 sec) internal and external pressure equilibrium. After the experiment, CO₂ was injected into the rock core at 5 atm to verify the presence of fractures connected to the external surface of the sample. CO₂ leakage was immediate and profuse on rock samples Coso 1-1 and 1-2 subjected to hydraulic fracturing with 1 wt% aqueous PAA and CO₂ (Fig. S13) and occurred within the top 2.54 cm of the rock core, consistent with the location of the center hole (2.54 cm depth) where the hydraulic fracturing fluid was injected (Fig. S14).

The results suggest that fracturing of a crystalline rock core at the above experimental conditions is only possible with PAA-CO₂ hydraulic fracturing fluid. Based on the rheology behavior of aqueous PAA-CO₂ fluid as a function of temperature (Fig. 1), aqueous PAA-CO₂ fluid is unlikely to form a gel at the experimental temperatures and pressures described above (210°C, 200–340 atm). Nonetheless, the aqueous PAA-CO₂ fluid generated fractures on the highly impermeable rock samples due to the CO₂-induced volume

expansion in a confined environment combined with rapid increase in fluid viscosity (Figs. 1 and 3). However, due to the resolution limit (voxel resolution = $\sim 30\text{--}35\ \mu\text{m}$) of the instrument XMT analysis was only able to identify the presence of local fractures with no connection to the external surface, even though the presence of fractures was evidenced by flowing CO_2 through the rock core (Fig. S13). These results indicate that the aperture of some of the fractures was smaller than $30\ \mu\text{m}$, and although they were large enough to allow fluid to flow through them, it was difficult to establish a clear map of the fracture network created. KI solution ($0.3\ \text{g/mL}$), which attenuates X-rays, was injected into the fractured rock cores (Coso 1-1 and 1-2) at 7 atm N_2 pressure. Seepage of KI solution was observed from the regions where CO_2 leakage occurred at 7 atm CO_2 applied pressure (Fig. S15). Based on the observed seepage velocity of $\sim 0.4\ \text{mm/s}$ at a pressure gradient of 6 atm (7 atm at the inlet and 1 atm at the outlet), the intrinsic permeability of the fractures formed

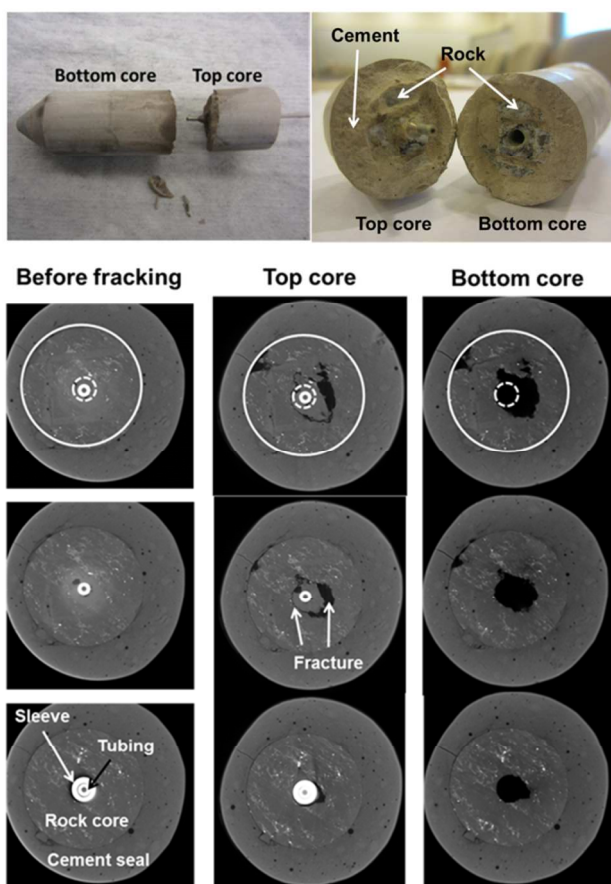


Fig. 3. Top. Pictures of Coso 2-2 core retrieved after hydraulic fracturing experiment. Both rock and cement seal were broken off, which resulted in a complete separation into two parts. **Bottom.** XMT horizontal slices of Coso 2-2 before and after hydraulic fracturing experiment with 1 wt% PAA- CO_2 at 210 °C and 272 atm confining pressure with 7 atm effective stress. After the experiment, XMT scanning was conducted by combining the two pieces (top and bottom core). The inner dashed circle indicates the size of the centered hole before hydraulic fracturing experiment, while the outer solid circle represents the diameter of the rock core. Cement slurry was placed between tubing and rock in the centered hole as well as on the external surface of the rock core for sealing purposes.

on Coso 1-2 was calculated using Darcy's law to be approximately $5 \times 10^{-15}\ \text{m}^2$ (5 mD), which is comparable to the typical permeability

of sandstone reservoir rocks [46]. After the injection of KI solution, the rock cores were scanned by XMT. However, no obvious fractures (e.g., bright lines due to KI filling) were visible, except for the bright regions on the outside surface of the rock cores where KI solution had leaked out (Fig. S16). The results suggest that most of the fractures formed by PAA and CO_2 are microfractures with aperture size $< 30\ \mu\text{m}$. Given the fact that 1 wt% PAA solution at the temperature and CO_2 pressures employed in the fracturing experiments shows volume expansion with no gel formation, higher temperatures and/or pressures may need to be applied to potentially create larger fractures that can be visualized by XMT analysis. Nevertheless, successful and reproducible hydraulic fracturing was demonstrated at significantly low effective stress, between 4 to 6 atm, while conventional fluids were not able to create fractures at considerably higher pressures applied.

Rock sample Coso 2-2

In order to increase the fluid viscosity and volume expansion in constrained environments one additional fracturing experiment with 1 wt% PAA solution was carried out at higher pressure. In this case, the temperature was similar to the temperature of the previous experiments (210°C) but the external confining pressure was nearly 70 atm higher (272 atm). Then, gradually increasing the internal fluid pressure to 279 atm (just 7 atm above the confining pressure) resulted in immediate equilibration of external and internal pressure (1-2 sec) which was caused by the complete rupture and separation of the cemented rock core (Coso 2-2) into two parts (Fig. 3). The separation took place near the top end of the rock core where the fracturing fluid was introduced. XMT images displayed that both rock and cement seal surrounding the tubing were fractured by the PAA- CO_2 fluid at 7 atm effective stress (Fig. 3 and Fig. 4). In addition, along the fractures formed in the cement seal, a zone with light color ($< \sim 0.5\ \text{mm}$ thick) was formed (Fig. 4). This is attributed to CaCO_3 precipitation in cement pores during the reaction between cement and CO_2 fluid flowing out to the external confining fluid through the large fractures [47]. Control experiments with pure water/ CO_2 and SDS 1wt% and CO_2 under identical pressure/temperature conditions showed no fracture creation even at differential pressures as high as 50 atm. It is important to note that the expected high localized pressures originated by volume expansion were not detected with the pressure transducers. This is due to the very small volumes of PAA-based fluid introduced ($300\ \mu\text{L}$) and the size of the resulting fractures ($20\text{--}30\ \mu\text{m} \times \sim 1\ \text{cm}$ length) which are insignificant volumes when compared to the dead volumes of the rest of the system including the pumps. Nevertheless, from the outcome of fracturing experiments observed on control experiments, the results demonstrate that the volume expansion in confined environments seems to be the source of large localized effective pressures and the resulting fractures formation.

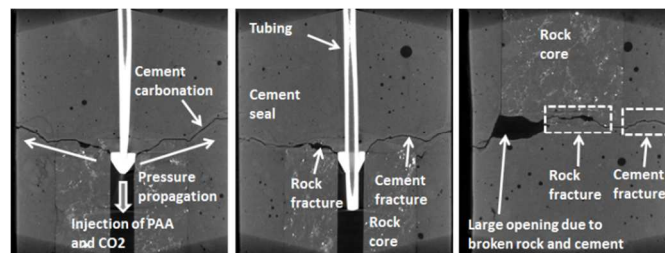


Fig. 4. XMT vertical slices of Coso 2-2 showing new fractures formation in rock and cement seal. Cement matrix along the fracture is carbonated (e.g., CaCO_3 precipitation in cement pores) as a result of the reaction with CO_2 fluid during the fracturing experiment.

CFD modeling and fracture network description on rock cores Coso 1-2 and Coso 2-2 geothermal field

Rock sample Coso 1-2

As described above, rock sample Coso 1-2 manifested microfractures with sizes smaller than 30 μm that were difficult to track down by XMT analysis. Nevertheless, comparison of Coso 1-2 sample before and after fracturing showed some local fractures with larger aperture that were able to be captured by XMT, but could not be modeled by CFD due to the resolution limit of the XMT instrument. Fig. S17 shows a 3D image of a local fracture confirming that aqueous PAA-CO₂ fluid can create fractures causing a dramatic overall increase in rock permeability as compared to the original rock sample as also demonstrated by the seepage KI experiment.

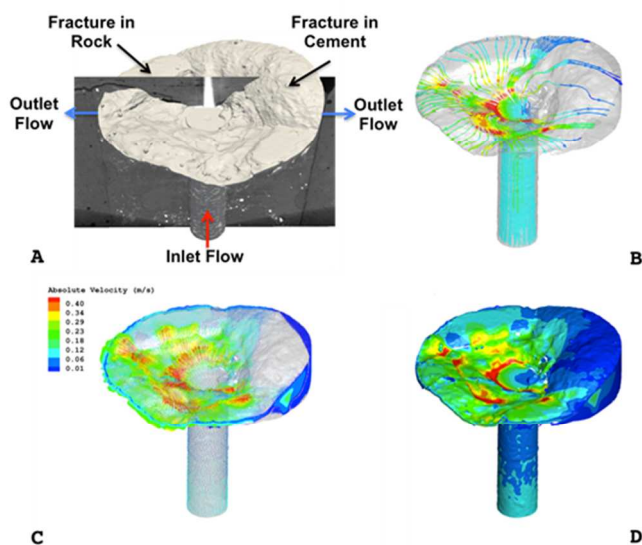


Fig. 5. (A) Isosurface of the fractures created in Coso 2-2 along with a vertical XMT slice. The center hole was considered to be the inlet of the 3D model, where flow was driven by specified velocity and the outlet was assumed to be the interface between the rock sample and the surrounding cement seal. (B) Stream-traces colored by absolute velocity. (C) and (D) represent velocity vectors colored by absolute velocity and contours of absolute velocity, respectively.

Rock sample Coso 2-2

CFD modeling on rock sample Coso 2-2 exhibited a significant increase in fluid flow and thus permeability due to new fractures generated by the hydraulic fracturing experiment performed using aqueous PAA-CO₂ fluid system. Due to the sample treatment and location of the hydraulic fractures, the fractures in the rock sample and cement seal region could not be differentiated (Fig. 5A). Hence, the 3D model for the CFD simulation and permeability computation consisted of fractures in both the rock and cement seal. Roughly, 63% of the model volume consisted of the fractured rock. Fig. 5B, 5C and 5D show stream traces, volumetric velocity vectors and contours colored by absolute velocity, respectively. Since the fracture formation is in the horizontal plane of the rock sample, the flow in the drill hole encounters a nearly 90° turn and enters the fracture, which has a smaller cross-sectional area. Due to the reduced cross-sectional area, the flow accelerates and this acceleration of flow is evident in Figs. 5B, 5C and 5D where high-speed velocity regions can be noticed around the drilled hole. From Figs. 5C and 5D, it can be noticed that the significantly reduced flow in the fracture located in the cement seal region. This could be attributed to

the fact that the connectivity between the fracture in the cement seal region and the drill hole is limited, thereby diverting the fluid into fractures in the rock sample region. Hence, we can notice more flow and higher fluid velocity in fractures located in the rock sample region compared to the fractures that originated in the cement region where the flow and fluid velocities are negligible (Fig. 5C and 5D). The overall fracture permeability of the sample was $1.81 \times 10^{-13} \text{ m}^2$ (180 mD). This represents a remarkable stimulation of the permeability in the core sample. The pre-fracturing permeability was too low to measure, and the post-fracturing permeability is comparable to a high-permeability aquifer (i.e., well-sorted gravel) [48].

It should be noted that the Coso geothermal field samples fractured in this work are mainly diorite rock samples, one of the strongest existing rocks with compressive strengths in the range of 1500-2000 atm.[49, 50] Hydrated Portland cement (water/cement ratio = 0.4) has compressive strength of ~ 350 atm which, although lower than diorite, it is still higher than most sedimentary rocks.[49, 51] In other words, the aqueous PAA-CO₂ fracturing fluid can reproducibly create fracture networks in low permeability rock demonstrating the exceptional potential of this fluid technology to increase reservoir permeability and enable the feasibility of EGS. This clearly shows that the CO₂-activation is key to the fracturing power of these fluids, thus showcasing new chemistry and enhanced fracturing potential compared to all comparable fluids used industrially.

Estimated environmental impact of the reported fluid

One of the primary environmental benefits of the PAA solutions is that in principle, any dissolved emulsions/gels can be recovered with the water and then treated on the surface and recycled or removed from the well. PAA solutions can be recovered by simple depressurization of CO₂ and/or by using any dilute acid (hydrochloric or sulfuric acid) as indicated by the work of Weiss et al.[36, 38] Weiss had shown that acid can liberate CO₂ from carbamate/bicarbonates in the gel, but acid also catalyzes the hydrolysis of urea bonds of the crosslinked PAA. We propose a more environmentally benign option utilizing acidic ion exchange resins, where the PAA solution could be filtered through the resin and PAA can be recovered. Any dissolved counterions or minerals in the brine can then be contained within the resins. Recovery and reactivation of the PAA is a current focus of study in our laboratory.

PAA solutions are not expected to contribute to any significant environmental damage and should pose little toxicity threat if it were to accumulate in a reservoir. PAA that accumulates within the rock may undergo thermal decomposition, though there is little to no published thermal or chemical degradation data available on PAA or its solutions. It should be noted that the hydrogel formed by CO₂-triggered crosslinking of the PAA appeared to be stable in our experiments at temperatures as high as 330 °C in our testing. If degradation were to occur, we anticipate thermal or chemical decomposition of the polymer into ammonia (which would be promptly converted to ammonium hydroxide or ammonium carbonate/bicarbonate and subsequently mineralized) and polypropylene. Some accumulation of polypropylene may occur in the rock, but no more than tailings from other polymers in conventional fracking fluids. Polypropylene is known to thermally decompose into alkanes and alkenes,[52, 53] which are likely to be present in the shale oil/gas trapped inside the fractured rock to begin with. Thus, we project that any decomposition product should cause little to no more environmental damage than that of the organics entailed in the rock prior to fracturing. A follow on study will focus

on chemical and thermal decomposition of the solutions and toxicity studies prior to injection in a live well.

Conclusions and implications for enhanced geothermal and hydrocarbons systems

This work reports for the first time a switchable hydraulic fracturing fluid that undergoes a reversible, large and fast (seconds) volume expansion with a simultaneous increase in viscosity triggered by CO₂ at temperatures relevant for reservoir stimulation in EGS. The main goal of this work is to demonstrate proof of concept on a novel fracturing fluid that can create a significantly large mechanical stress in the confined environments of the fracture networks, specifically at EGS depths of interest, creating fractures at effective stress at least an order of magnitude lower than current technology. Although the actual measurement of the pressure “spike” was not determined, due to the degree of complexity and technical challenge this measurement entails, the remarkable performance of the fluid system was demonstrated by carrying out high pressure/temperature laboratory-scale experiments that simulated reservoir stimulation conditions at different depths (different confining P and T) on actual EGS reservoir samples. Fracture creation with the corresponding permeability enhancement was successfully achieved with minimum effective stress (4-7 atm, an order of magnitude lower than conventional fracturing fluids) independently of the confinement pressure. Aqueous PAA-CO₂ mixtures also showed significantly higher viscosities than conventional rheology modifiers at similar pressures and temperatures due to the cross-linking reaction of PAA with CO₂, which was demonstrated by chemical speciation studies using *in situ* HP-HT ¹³C MAS-NMR. In addition, PAA shows shear-thinning behavior, an additional critical advantage for the use of this fluid system in reservoir stimulation; shear-thinning supports fluid propagation and proppant transport into the reservoir at high shear rates.

This study also demonstrates that PAA-CO₂ fluid systems are rheoreversible (e.g., liquid to gel and gel to liquid)[37] by adjusting the CO₂ pressure. Alternatively, the hydrogel can be converted into a liquid with the addition of any diluted acid.[42] Although a thorough study (which is outside the scope of the present work) is required to learn about the potential recovery of these fluids after proppant emplacement, the rheoreversible behavior of PAA suggest the feasibility of removal of the hydraulic fracturing polymers from geothermal reservoirs during post-fracturing cleanup. This could be done by converting the hydrogel to a liquid PAA solution that can be pumped back to the surface for recycling. These features demonstrate the potential of CO₂-reactive rheoreversible hydraulic fracturing fluids to increase energy production from EGS reservoirs while minimizing reservoir creation cost and environmental impact. For this proposed alternative method to conventional fracturing, PAA would be injected in series followed by injection of CO₂. PAA can then be removed upon CO₂ depressurization or injection of a weak acid. This will eliminate the need to use shear thinning fluids (xanthan or guar gum), surfactants (SDS), cross linkers and breakers. PAA is also an antioxidant and biocide which will replace the use of common corrosion inhibitors such as formic acid and biocides such as chlorine. Since PAA-CO₂ hydraulic fracturing fluids could create/propagate fracture networks more efficiently than current technology (owing to the described additional stress created during volume expansion), environmental problems associated with a large volume of flowback water will be reduced. This is because significantly lower volumes of water will be required for reservoir stimulation, decreasing the volume of wastewater produced. As mentioned earlier, removing injected chemicals from the subsurface after fracturing, which is the intent of stimu-

responsive/rheoreversible hydraulic fracturing fluids, decreases environmental risks. However, there are other risks associated with fracturing such as induced seismicity and contamination of ground water due to solubilisation of minerals) that this technology cannot address (although the authors can argue that minerals dissolution will be decreased due to the predicted lower volumes of water required to fracture in the first place).

PAA-CO₂ fracturing fluid can also be potentially employed for unconventional oil and gas recovery. For tight oil recovery, low-intermediate molecular weight, water-soluble polymers will be employed to gel under moderate temperatures and high pressures (>60°C, >300atm). A high-degree of crosslinking will promote gel formation, which will significantly increase the viscosity and alter the rheological properties of the fracturing fluid to create fractures. However, during gel solubilization and removal (for recycling) in free-surfactant form, a low viscosity solution surfactant will be preferred, so that emulsions of the oil can be pumped and recovered at the surface.

In brief, this work reports a novel fracturing fluid that: (1) increases viscosity at EGS high temperatures and pressure (conventional gels would degrade), (2) can be potentially cleaned out with depressurization and/or diluted acid injection, (3) is a more environmentally friendly alternative to standard methods, and (4) it significantly lowers the fracture initiation pressure in highly impermeable crystalline rock as compared to conventional fracturing fluids. Energy production needs continue to grow. While hydraulic fracturing entails potential risks and significant environmental impacts, stimuli-responsive (chemically reactive/potentially recyclable) fracturing fluids are an alternative that provides reduced environmental risk with concomitant highly effective permeability stimulation, which could make EGS competitive with hydrocarbons in the energy market and unconventional oil/gas exploitation cost-effective and cleaner.

Acknowledgements

We are grateful to Joseph Moore at Energy & Geoscience Institute for providing rock cores from the Coso geothermal field, Dr. Maura Zimmerschied and Dr. Steven Wiley for very useful edits and suggestions. XMT, and NMR analysis was performed in EMSL (Environmental Molecular Sciences Laboratory; EMSL proposal # 47743), a DOE national scientific user facility at Pacific Northwest National Laboratory (PNNL). Funding for this research was provided by the Geothermal Technology Office of the U.S. Department of Energy. Pacific Northwest National Laboratory is operated by Battelle for the U.S. Department of Energy under contract DE-AC06-76RLO 1830.

Notes and references

^a Pacific Northwest National Laboratory, Richland, WA 99352.

^b New Mexico State University, Las Cruces, NM 88003.

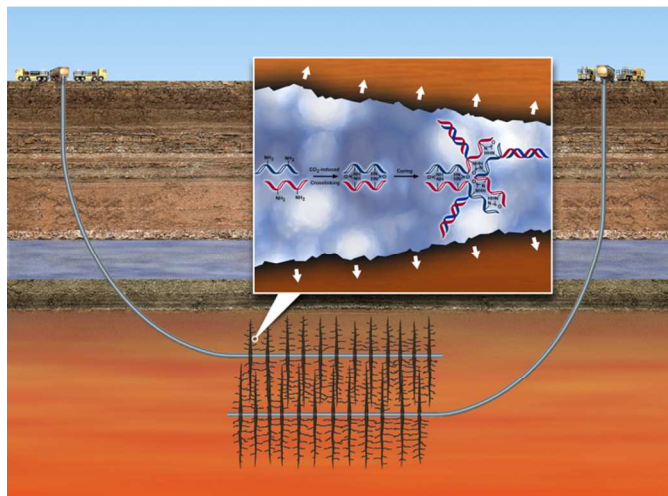
† Electronic Supplementary Information (ESI) available: Schematic diagram and photos of HP-HT experimental setup, HP cell temperature calibration, pictures of polymer-CO₂ mixtures and water-CO₂ mixture, viscosity of DIW-CO₂ mixture, hydraulic fracturing experimental setup and XMT images are included in the supporting information.]. See DOI: 10.1039/b000000x/

[1] Blackwell DD, Negraru PT, Richards MC. Assessment of the Enhanced Geothermal System Resource Base of

- the United States. *Natural Resources Research* 2006;15:283-303.
- [2] Duffield WA, Sass JH. Geothermal energy - Clean power from the Earth's heat. *U.S. Geol. Surv. Circ.*, 1249; 2003.
- [3] Pruess K. Enhanced geothermal systems (EGS) using CO₂ as working fluid - A novel approach for generating renewable energy with simultaneous sequestration of carbon. *Geothermics* 2006;35:351-67.
- [4] Kargbo DM, Wilhelm RG, Campbell DJ. Natural Gas Plays in the Marcellus Shale: Challenges and Potential Opportunities. *Environmental Science & Technology* 2010;44:5679-84.
- [5] Kerr RA. Natural Gas From Shale Bursts Onto the Scene. *Science* 2010;328:1624-6.
- [6] Scotchman IC. Fracking: Royal Society of Chemistry; 2015.
- [7] Dake LP. *Fundamentals of Reservoir Engineering*: Elsevier, Amsterdam; 1978.
- [8] Baria R, Baumgartner J, Gerard A, Jung R, Garnish J. European HDR research programme at Soultz-sous-Forets (France) 1987-1996. *Geothermics* 1999;28:655-69.
- [9] Rushing JA, Sullivan RB. Evaluation of hybrid water-frac stimulation technology in the bossier tight gas and play. SPE Annual Technical Conference and Exhibition, 5-8 October. Denver, Colorado Society of Petroleum Engineers; 2003.
- [10] Jones CG, Simmons SF, Moore JN. Proppant Behavior Under Simulated Geothermal Reservoir Conditions. Proceedings, Thirty-Ninth Workshop on Geothermal Reservoir Engineering. Stanford University, Stanford, California February 24-26, 2014.
- [11] McLin K, Brinton D, Moore JN. The Chemical and Thermal Stability of Proppants under Geothermal Conditions. AAPG/SPE/SEG Hedberg Research Conference "Enhanced Geothermal Systems" Napa, California March 14-18, 2011.
- [12] Shiozawa S, McClure M. EGS Designs with Horizontal Wells, Multiple Stages, and Proppant. Proceedings, Thirty-Ninth Workshop on Geothermal Reservoir Engineering. Stanford University, Stanford, California February 24-26, 2014.
- [13] Tollefson J. Secrets of fracking fluids pave way for cleaner recipe. *Nature* 2013;501:146-7.
- [14] Jang BN, Costache M, Wilkie CA. The relationship between thermal degradation behavior of polymer and the fire retardancy of polymer/clay nanocomposites. *Polymer* 2005;46:10678-87.
- [15] Wang M, Smith JM, McCoy BJ. Continuous kinetics for thermal-degradation of polymer in solution *AIChE Journal* 1995;41:1521-33.
- [16] Garcia-Ochoa F, Santos VE, Casas JA, Gomez E. Xanthan gum: production, recovery, and properties. *Biotechnology Advances* 2000;18:549-79.
- [17] Gallup DL. Production engineering in geothermal technology: A review. *Geothermics* 2009;38:326-34.
- [18] Jessop PG, Mercer SM, Heldebrant DJ. CO₂-triggered switchable solvents, surfactants, and other materials. *Energy & Environmental Science* 2012;5:7240-53.
- [19] O'Neill C, Fowler C, Jessop P, Cunningham M. Redispersing aggregated latexes made with switchable surfactants. *Green Materials* 2014;1:27-35.
- [20] Su X, Cunningham MF, Jessop PG. Use of a switchable hydrophobic associative polymer to create an aqueous solution of CO₂-switchable viscosity. *Polymer Chemistry* 2014;5:940-4.
- [21] Su X, Cunningham MF, Jessop PG. Switchable viscosity triggered by CO₂ using smart worm-like micelles. *Chem Commun* 2013;45:2655-7.
- [22] Han D, Boissiere O, Kumar S, Tong X, Tremblay L, Zhao Y. Two-Way CO₂-Switchable Triblock Copolymer Hydrogels. *Macromolecules* 2012;45:7440-5.
- [23] Han D, Tong X, Boissiere O, Zhao Y. General Strategy for Making CO₂-Switchable Polymers. *ACS Macro Letters* 2012;1:57-61.
- [24] Zhang Y, Chu Z, Dreiss CeA, Wang Y, Feiac C, Feng Y. Smart wormlike micelles switched by CO₂ and air. *Soft Matter* 2013;9:6217-21.
- [25] Zhang Y, Feng Y, Wang Y, Li X. CO₂-Switchable Viscoelastic Fluids Based on a Pseudogemini Surfactant. *Langmuir* 2013;29 4187-92.
- [26] Zhang Y, Yujun Feng, Wang J, He S, Guo Z, Chua Z, et al. CO₂-switchable wormlike micelles. *Chem Commun* 2013 49:4902--4
- [27] Shchukin D, Mohwald H, Guerreiro M, Ferreira S, Zheludkevich M. Corrosion inhibiting pigment comprising nanoreservoirs of corrosion inhibitor 2009.
- [28] Iarikov DD, Kargar M, Sahari A, Russel L, Gause KT, Behkam B, et al. Antimicrobial Surfaces Using Covalently Bound Polyallylamine. *Biomacromolecules* 2014;15:169-76.
- [29] Hoyt DW, Turcu RVF, Sears JA, Rosso KM, Burton SD, Felmy AR, et al. High-pressure magic angle spinning

- nuclear magnetic resonance. *Journal of Magnetic Resonance* 2011;212:378-85.
- [30] Turcu RVF, Hoyt DW, Rosso KM, Sears JA, Loring JS, Felmy AR, et al. Rotor design for high pressure magic angle spinning nuclear magnetic resonance. *Journal of Magnetic Resonance* 2013;226:64-9.
- [31] Carson JP, Einstein DR, Minard KR, Fanucchi MV, Wallis CD, Corley RA. High resolution lung airway cast segmentation with proper topology suitable for computational fluid dynamic simulations. *Computerized Medical Imaging and Graphics* 2010;34:572-8.
- [32] Carson JP, Kuprat AP, Jiao X, Dyedov V, Del Pin F, Guccione JM, et al. Adaptive generation of multimaterial grids from imaging data for biomedical Lagrangian fluid-structure simulations. *Biomechanics and modeling in mechanobiology* 2010;9:187-201.
- [33] Lorensen WE, Cline HE. Marching cubes: A high resolution 3D surface construction algorithm. *ACM SIGGRAPH Computer Graphics* 1987;21:163-9.
- [34] Kuprat A, Khamayseh A, George D, Larkey L. Volume conserving smoothing for piecewise linear curves, surfaces, and triple lines. *Journal of Computational Physics* 2001;172:99-118.
- [35] Kuprat AP, Einstein DR. An anisotropic scale-invariant unstructured mesh generator suitable for volumetric imaging data. *Journal of Computational Physics* 2009;228:619-40.
- [36] Carretti E, Dei L, Baglioni P, Weiss RG. Synthesis and characterization of gels from polyallylamine and carbon dioxide as gellant. *Journal of the American Chemical Society* 2003;125:5121-9.
- [37] Carretti E, Dei L, Macherelli A, Weiss RG. Rheoreversible polymeric organogels: The art of science for art conservation. *Langmuir* 2004;20:8414-8.
- [38] Carretti E, Dei L, Weiss RG. Soft matter and art conservation. *Rheoreversible gels and beyond*. *Soft Matter* 2005;1:17-22.
- [39] Guo Z, Feng Y, Wang Y, Wang J, Wu Y, Zhang Y. A novel smart polymer responsive to CO₂. *Chemical Communications* 2011;47:9348-50.
- [40] Heldebrant DJ, Koech PK, Ang MTC, Liang C, Rainbolt JE, Yonkera CR, et al. Reversible zwitterionic liquids, the reaction of alkanol guanidines, alkanol amidines, and diamines with CO₂. *Green Chem* 2010;12:713-21.
- [41] Yu T, Wakuda K, Blair DL, Weiss RG. Reversibly Cross-Linking Amino-Polysiloxanes by Simple Triatomic Molecules. *Facile Methods for Tuning Thermal, Rheological, and Adhesive Properties*. *Journal of Physical Chemistry C* 2009;113:11546-53.
- [42] Carretti E, Bonini M, Dei L, Berrie BH, Angelova LV, Baglioni P, et al. *New Frontiers in Materials Science for Art Conservation: Responsive Gels and Beyond*. *Accounts of Chemical Research* 2010;43:751-60.
- [43] Huenges E, Holl HG, Legarth B, Zimmermann G, Saadat A. The stimulation of a sedimentary geothermal reservoir in the north German basin: Case study Groß Schönebeck. *Proceedings, Twenty-Ninth Workshop on Geothermal Reservoir Engineering*. Stanford University, Stanford, California January 26-28, 2004.
- [44] Mader D. *Hydraulic Proppant Fracturing and Gravel Packing*. Amsterdam: Elsevier; 1989.
- [45] Pinto ML, Mafra L, Guil JM, Pires J, Rocha J. Adsorption and Activation of CO₂ by Amine-Modified Nanoporous Materials Studied by Solid-State NMR and (CO₂)-C-13 Adsorption. *Chemistry of Materials* 2011;23:1387-95.
- [46] Pape H, Clauser C, Iffland J. Permeability prediction based on fractal pore-space geometry. *Geophysics* 1999;64:1447-60.
- [47] Jung HB, Jansik D, Um W. *Imaging Wellbore Cement Degradation by Carbon Dioxide under Geologic Sequestration Conditions Using X-ray Computed Microtomography*. *Environ Sci Technol* 2013;47:283-9.
- [48] Fetter CW. *Applied Hydrogeology*. 4th ed: Prentice Hall; 2001.
- [49] Berkman DA. *Field geologist's manual* 4th ed: The Australasian Institute of Mining and Metallurgy, Australia; 2001.
- [50] Davatzes NC, Hickman SH. *Stress and faulting in the Coso Geothermal Field: update and recent results from the East Flank and Coso Wash*. Stanford University, Stanford, CA, Jan 30-Feb 1, SGP-TR-179: 31st workshop on Geothermal Reservoir Engineering, Stanford University, Stanford, CA; 2006.
- [51] Guettala S, Mezghiche B. Compressive strength and hydration with age of cement pastes containing dune sand powder. *Construction and Building Materials* 2011;25:1263-9.
- [52] Bockhorn H, Hornung A, Hornung U, Schawaller D. Kinetic study on the thermal degradation of polypropylene and polyethylene. *Journal of Analytical and Applied Pyrolysis* 1999; 48 93-109.
- [53] Davis TE, Tobias RL, Peterli EB. Thermal degradation of polypropylene. *Journal of Polymer Science* 1962;56:485-99.

Highlights figure/Suggested cover art



ARTICLE

Stimuli-Responsive/Rheoreversible Hydraulic Fracturing Fluids as an Alternative to Support Geothermal and Fossil Energy Production

Table of Contents

A reversible CO_2 -triggered volume expansion significantly lowers the fracture initiation pressure in highly impermeable crystalline rock as compared to conventional fracturing fluids

